Progress In Electromagnetics Research, Vol. 168, 61–71, 2020

Polarization Reconfigurable Slot-Fed Cylindrical Dielectric Resonator Antenna

Mahbubeh Esmaeili* **and Jean J. Laurin**

Abstract—A new design for a cylindrical dielectric resonator antenna (DRA) with a capability of switching between circular, linear horizontal and linear vertical polarizations is introduced. The DRA, operating at the center frequency of 3.25 GHz, is fed by a microstrip line through two dog-bone slots. In this design, only two PIN diodes are employed as switching elements which significantly decreases the complexity of DC biasing circuits compared to existing designs. The PIN diodes are embedded in transformers connected to the feeding microstrip lines. This technique conveniently allows to make compensations for parasitic effects of the PIN diodes junction capacitors on the antenna matching bandwidth. The circular, linear horizontal and linear vertical polarizations have a bandwidth of 22%, 17% and 18%, respectively. The 3-dB axial ratio bandwidth for the circular polarization is 12%. The measured results obtained from prototyped antenna agree well with simulated results of the designed antenna system, which confirms the validity of the design process.

1. INTRODUCTION

Reconfigurable polarization antennas allow switching between different communication systems working with different antenna polarizations. In addition, in a single communication network, employing a reconfigurable polarization antenna allows to select the best polarization depending on transmitting and receiving circumstances to maintain the quality of service. For example in satellite communications, circular polarization (CP) is the best choice to reduce the miss-match polarization losses in receivers. Reconfigurable polarization antennas are widely used in software defined radios (SDRs) and vehicular communication systems. Simplicity of the switching network, the number of switching elements and their losses, matching and axial ratio bandwidth of the antenna system are key points in the reconfigurable polarization antenna design process.

A lot of research has been conducted on switchable polarization antennas using three main techniques. A conventional method consists of simply switching between antennas with different polarizations [1]. This technique is not so interesting because it leads to non-compact antenna systems. As the second method, radiators can be altered appropriately, such as truncating and etching slots on them, with some switches to change the antenna polarization [2–5]. In this case, the switching elements are directly connected to antennas and can affect the antenna properties such as radiation pattern, gain and efficiency due to their parasitic elements. A third method to have polarization reconfigurability is designing a reconfigurable feeding system for an antenna to change the antenna polarization [6–9], without changing the radiation element itself. This leads to more compact designs compared to the first method. Also, compensating for the diode parasitics can be done without affecting the pattern. This approach has been used in this work.

Received 12 April 2020, Accepted 9 July 2020, Scheduled 15 October 2020
* Corresponding author: Mahbubeh Esmaeili (mahbubeh.esmaeili@polymtl.ca).
The authors are with the Poly-Grames Research Center, Electrical Engineering Departement, Polytechnique Montreal, Montreal, QC, Canada.

Reconfigurable dielectric resonator antennas (DRAs) are interesting due to their higher power handling and compact size compared to their microstrip patch counterparts. The earliest reconfigurable polarization DRA is reported in [10]. In this design, PIN diode switches are in parallel with microstrip feeding lines and the antenna bandwidth is limited by the effect of junction capacitors of PIN diodes. The Bandwidths for 7-dB return loss are reported about 4% and 3% for circular and linear polarizations antennas, respectively. Although, other types of switchable DRA antennas were reported later such as [11–14], to our best knowledge, none of them has addressed the bandwidth limitation of the DRA reported in [10].

The dual-probe fed cylindrical DRA in [11] generates two linear polarizations (LPs) and two circular polarizations (CPs) using eight PIN diodes. Although a very large bandwidth of 30% is reported for LPs, the matching bandwidth of two CPs are 6.3% and 9.5%. Therefore, the overlapped bandwidth is limited to 6.3%. The glass dielectric resonator antenna reported in [12] has a good overlapped bandwidth of 18%, but it generates three states of linear polarization and no circular polarization. Polarization reconfigurability is achieved by injecting a liquid metal polarizer into two microfluidic channels sandwiched between two pieces of the glass DRA which makes the switching procedure slow. In [13], a reconfigurable polarization glass cylindrical DRA is presented that can produce three polarization states as the same those reported in [12], by integrating a metallic polarizer in the DRA. In this design, the polarizer is a planar metallic structure loaded with four PIN diodes. Since the polarizer, diodes, and their biasing circuits are located between two pieces of the DRA, the antenna structure is complex. A good overlapped bandwidth of 15% has been reported for this antenna. The reconfigurable polarization antenna presented in [14] produces two linear and two circular polarizations by employing eight PIN diodes, but the overlapped bandwidth of the system is limited to 5%.

In this paper, we present a new feeding configuration for a cylindrical DRA which alleviates the bandwidth limitation of the antenna presented in [10], with the ability of switching between two linear and one circular polarizations, which makes the designed DRA superior to those presented in [12] and [13]. The overlapped bandwidth of 12% obtained for the three polarizations is comparable with those reported in [11] and [13]. In this configuration, switching PIN diodes are embedded in transformers, and transformers are connected to the feeding system, adopting the technique presented in [15]. Since only two PIN diodes are included in the feeding circuit, the antenna system is simpler compared to those reported in [11, 13, 14]. In addition, the switching procedure for the antenna is faster than that for the antenna presented in [12]. In this technique, the junction capacitor of PIN diodes in reversed-bias state has negligible effect on the antenna matching bandwidth. Therefore, even inexpensive PIN diodes with large junction capacitors can be employed.

2. ANTENNA DESIGN PROCESS

A cylindrical dielectric resonator antenna is designed to generate HEM_{111} mode and operate at the center frequency of $f_0 = 3.25\,\text{GHz}$ using [16]:

$$f_0 = \frac{c}{2\pi a\sqrt{\epsilon_r}}\left[1.71 + 2\frac{a}{h} + 0.1578\left(\frac{a}{h}\right)^2\right] \tag{1}$$

where c is the light speed in vacuum, and $\epsilon_r = 4$ is the dielectric constant of the DRA. The height and radius of the DRA are presented by h and a, respectively, which are $a = 17.40\,\text{mm}$ and $h = 25.40\,\text{mm}$ for the designed antenna.

Two orthogonal linear polarizations are created using two orthogonal slots, etched on the ground plane of a Rogers RO4003C substrate with the dielectric constant of $\epsilon_r = 3.55$ and thickness of $h_s = 1.524\,\text{mm}$, fed by two microstrip lines, as shown in Fig. 1. Port 1 generates linear horizontal polarization (LHP) in x direction by feeding slot 1, while port 2 excites linear vertical polarization (LVP) in y direction by feeding slot 2. The dimensions and positions of the slots are optimized to achieve the maximum matching bandwidth. Circular polarization (CP) is obtained by the superposition of LHP and LVP waves having the same amplitude and a relative phase of 90 degrees. For the antenna presented in this paper, this is achieved with a feeding network that splits the input signal into two signals of equal magnitude and by introducing a fixed 90° phase difference between them with a section of microstrip line. Feeding these signals to ports 1 and 2 in Fig. 1 will result in a CP wave in one handedness at the

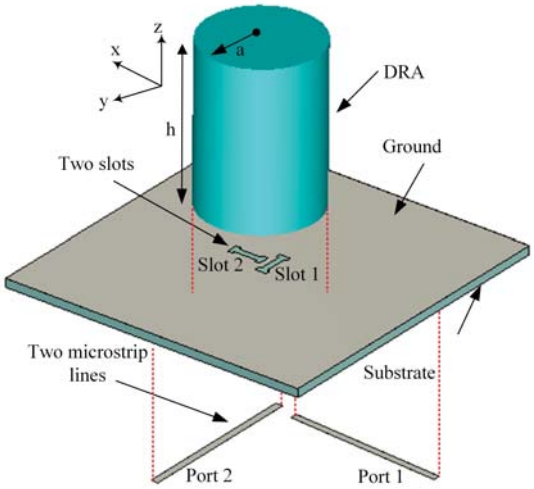

Figure 1. Designed dual-fed dielectric resonator antenna.

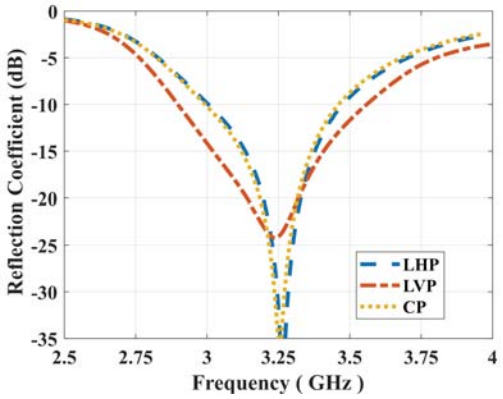

Figure 2. Simulated reflection coefficients of LHP, LVP, and CP of the two-port DAR depicted in Fig. 1.

design frequency. The simulated reflection coefficients for LHP, LVP, and CP of the designed antenna, illustrated in Fig. 1, are presented in Fig. 2. The simulated reflection coefficient for CP shown in Fig. 2 is the active reflection coefficient at port 1 when ports 1 and 2 are excited simultaneously with the same amplitude and 90° phase difference. The maximum realized simulated gain for all three polarizations is about 6 dB. No switches are used in these simulation, so the performance is only dependent on the DRA and coupling slots. A 10-dB return loss bandwidth of 15% (3–3.5 GHz) is obtained for all three polarizations.

The next section describes the design details of a new feeding topology with the ability of switching between LHP, LVP, and CP for the antenna presented in Fig. 1, employing PIN diodes as switching elements.

3. FEEDING SYSTEM WITH PIN DIODE SWITCHES

A simplified model for a PIN diode used as a switching element consists in a capacitor C_j in parallel with a large resistor, R_p, and a small resistor R_s in Off and On states, respectively, see Fig. 3. The component L_s is a packaging inductor. If PIN diodes are directly connected in series or in shunt with transmission lines, their junction capacitances can degrade the matching bandwidths when diodes are in Off states. To overcome this limitation, the topology presented in [15] is adopted. In this topology, diodes are embedded in a transformer network consisting of two transmission line sections, L_1 and L_2, as presented in Fig. 4(a).

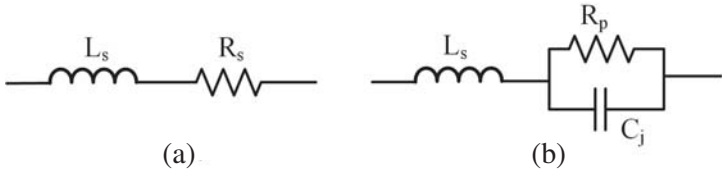

Figure 3. Equivalent circuit of a PIN diode: (a) forward bias (On state); (b) reversed bias (Off state).

The open impedance at the upper end of L_2 in Fig. 4(a) is transformed to Z_{t2} as purple line shows in Fig. 4(b). If diode D is On (low impedance), the impedance Z_{t2} is transformed along the strait red line to Z_{t1}, and then Z_{t1} is transformed to the open impedance point on Smith Chart, by L_1. The

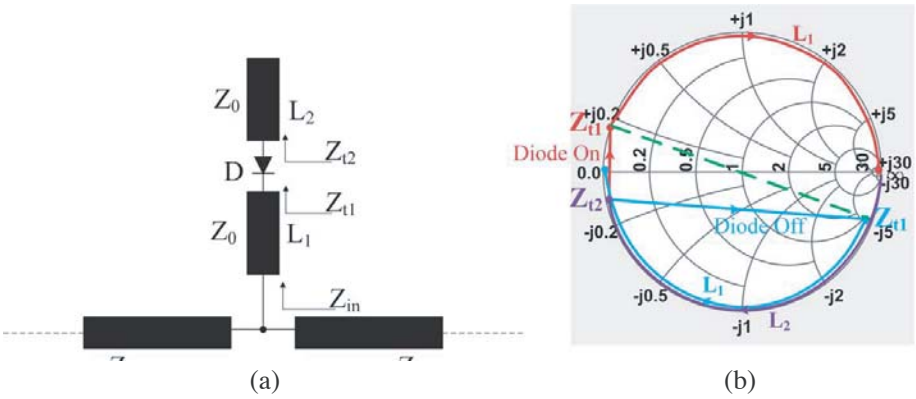

(a) (b)

Figure 4. (a) A PIN diode embedded in a transformer consisting of two transmission line sections L_1 and L_2. (b) Impedance transformation steps on Smith Chart.

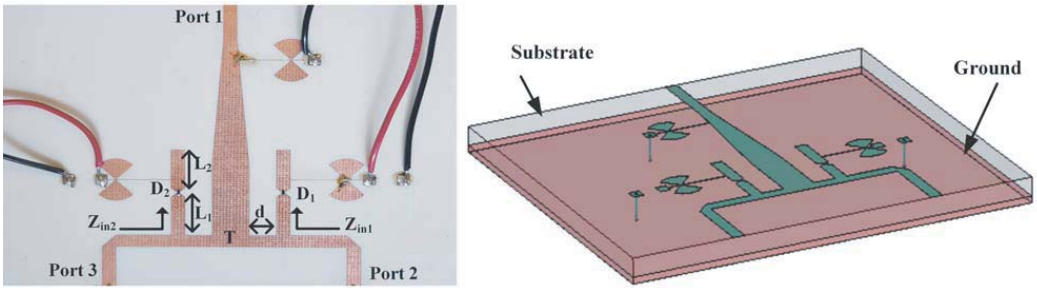

(a) (b)

Figure 5. Feeding system for the polarization reconfigurable DRA with two PIN diodes embedded in two transformers: (a) top view; (b) 3D view.

transformation from Z_{t1} to an infinite Z_{in} is represented as the red arc along the edge of the chart. If diode D is Off, Z_{t2} is transformed along the strait blue line to Z_{t1}, and then Z_{t1} is transformed into Z_{in} near the short circuit impedance point with the line section L_1, represented by the blue arc along the edge of the chart. The length of the transformer part L_2 is chosen appropriately so that the green line connecting the two Z_{t1} impedances passes through the Smith Chart center. Then, the segment of length L_1 transforms these two Z_{t1} states into two Z_{in} values that are as close as possible to zero and infinity. Therefore when diode D is Off the impedance Z_{in} is close to zero, and when the diode D is On, this impedance tends to infinity as shown in Fig. 4(b).

Although a transformer is designed for a specific values of C_j and R_s, since the transformers are wideband, a large group of PIN diodes with different junction capacitors and forward-bias resistors can be used in the transformer without significant effect on the matching bandwidth. A prototype of the feeding circuit for the reconfigurable polarization DRA antenna is shown in Fig. 5(a) with the DC biasing for two SMP1345-040LF Skyworks commercial PIN diodes with $L_s = 0.45\,\text{nH}$, $C_j = 0.2\,\text{pF}$, and $R_s = 2\,\Omega$ embedded in the transformer shown in Fig. 4. The feeding system is designed to operate at center frequency of 3.25 GHz. Table 1 summarizes different combinations of the diodes states, the simulated Z_{in1} and Z_{in2} input impedances, and their corresponding polarizations.

The input microstrip line at port 1 is tapered from $50\,\Omega$ to $25\,\Omega$ to minimize the mismatch at the T junction point for the circular polarization when both diodes are On. The parameters L_1 and L_2 are optimized to reach the maximum bandwidth at the goal frequency band of 3 GHz to 3.5 GHz. In addition, the distance d between each transformer and T junction is optimized to maximize the matching bandwidth for two linear polarizations when one of the diodes is On and the other is Off. The optimized values are $L_1 = 10\,\text{mm}$, $L_2 = 10.5\,\text{mm}$, and $d = 7\,\text{mm}$.

Table 1. Diodes' states in feeding circuit presented in Fig. 5 for generating different polarizations.

D_1	D_2	Z_{in1} (Ω)	Z_{in2} (Ω)	Polarization
On	On	200	200	CP
Off	On	5	200	LHP
On	Off	200	5	LVP

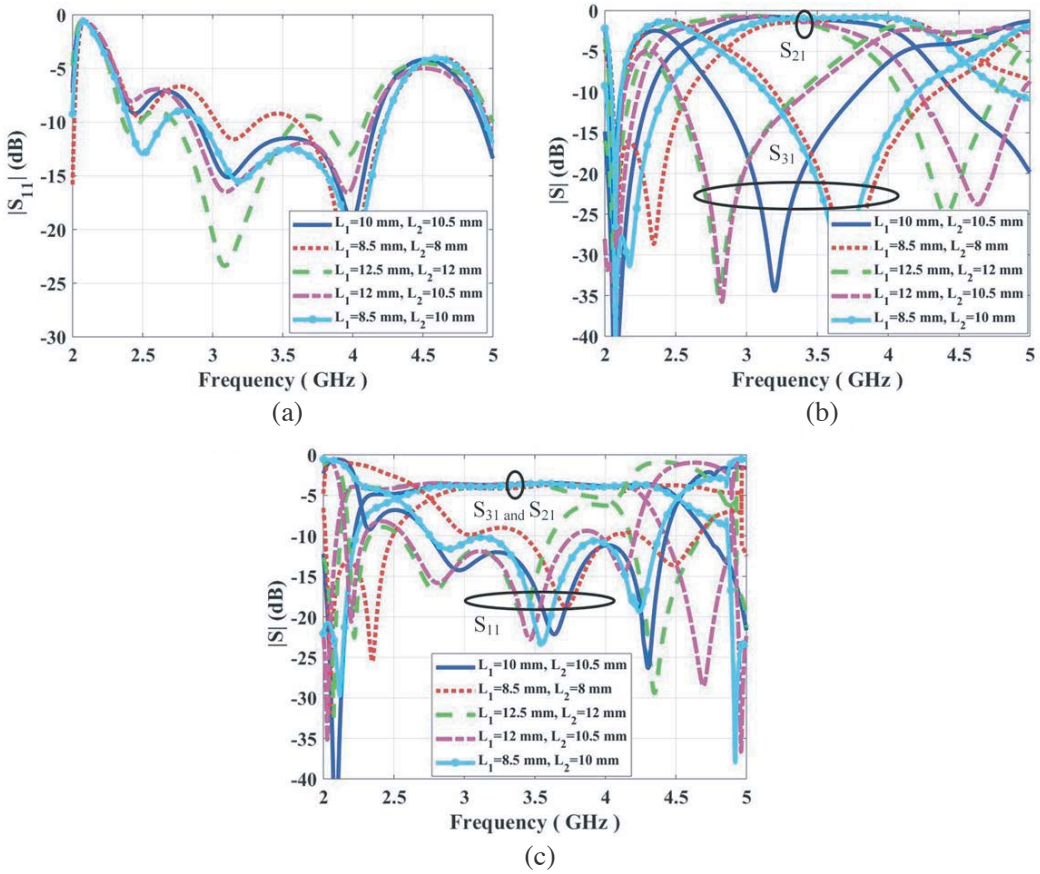

Figure 6. Variation of L_1 and L_2 and their effect on: (a) S_{11} when D_1 is On and D_2 is Off; (b) S_{21} and S_{31} when D_1 is On and D_2 is Off; (c) S_{11}, S_{21} and S_{31} when both D_1 and D_2 is On.

The effects of variation of L_1 and L_2 on the working bandwidth of the circuit shown in Fig. 5 are presented in Fig. 6. The most sensitive parameter is the coupling between the input port and the isolated port in the linear polarization mode (See parameter S_{31} in Fig. 6(b)). Proper adjustment of L_1 and L_2 brings the desired high-isolation operation in the frequency band of interest. More details of the designed feeding and biasing system are shown in Fig. 5(b). The butterfly patch closer to the port 1 is connected to the ground plane through a plated via hole which is the reference voltage for DC biasing. Two other grounded plated vias are used as reference voltage for D_1 and D_2. The two butterfly patches connected to line sections L_2 provide DC voltages for two PIN diodes.

When D_1 and D_2 are On simultaneously, Z_{in1} and Z_{in2} tend to infinity. Therefore, the power from port 1 is divided equally between ports 2 and 3 at the T junction point, which is necessary for generating circular polarization. When D_1 is On and D_2 is Off, port 3 is isolated by short-circuited Z_{in2} and the input power goes from port 1 to port 2, generating a linear polarization.

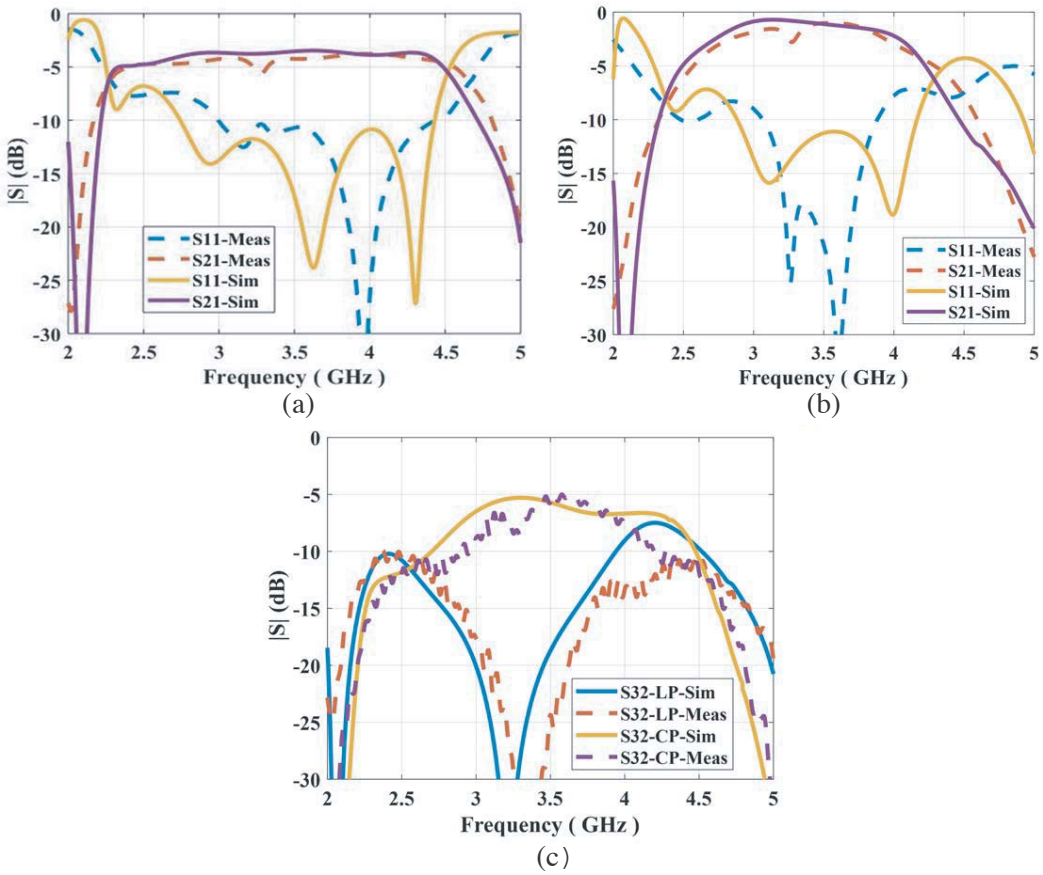

Figure 7. Switching performances of the PIN diodes in Fig. 5: (a) D_1 and D_2 are On; (b) D_2 is Off and D_1 is On; (c) isolation between ports when the feeding circuit is used to create linear polarization (LP) and circular polarization (CP).

The simulation results compared to experimental results for the circuit shown in Fig. 5 are presented in Fig. 7. When both diodes are On, a maximum insertion loss of 1.4 dB (in addition to the 3 dB due to power division) is measured, Fig. 7(a). The notch at 3.3 GHz, which is observed in [17] using the same diode, is attributed to the diode and its equivalent model. The results can be improved by choosing other commercial diodes. In the targeted bandwidth, a maximum insertion loss of 1.7 dB is measured when only port 2 is active (D_2 is On and D_1 is Off) as shown in Fig. 7(b). The losses are mainly attributed to the PIN diodes and to the microstrip lines. A good isolation between port 2 and port 3 is obtained when only one of them is active to generate a LP as presented in Fig. 7(c). In the case of CP, isolation between port 2 and port 3 should be very poor as depicted in Fig. 7(c), but the DRA is well matched for the two linear polarizations, so there is not much signal coming back in the feeding system. There are coaxial connector losses in addition to the other mechanisms.

4. RECONFIGURABLE POLARIZATION DRA: PROTOTYPING AND MEASUREMENT

In this section, the antenna designed in Section 2 is connected to the feeding network designed in Section 3 to realize a reconfigurable polarization antenna. The front view and the back view of the designed antenna are presented in Fig. 8(a) and Fig. 8(b), respectively. The antenna has only one RF port and two DC biasing ports. Labels "Port 2" and "Port 3" in Fig. 8(a) refer to the positions of these RF ports in Fig. 5(a). In Fig. 8(a), the two line segments going from the T-junction to the DRA

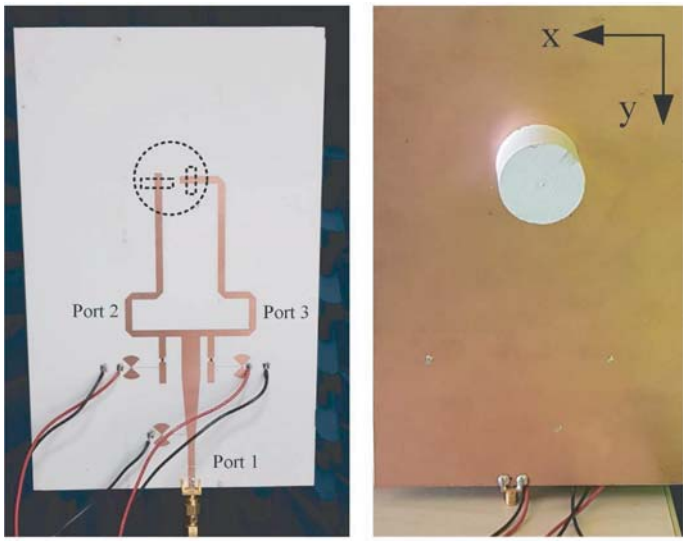

Figure 8. Fabricated reconfigurable polarization cylindrical dielectric resonator antenna: (a) front view; (b) back view.

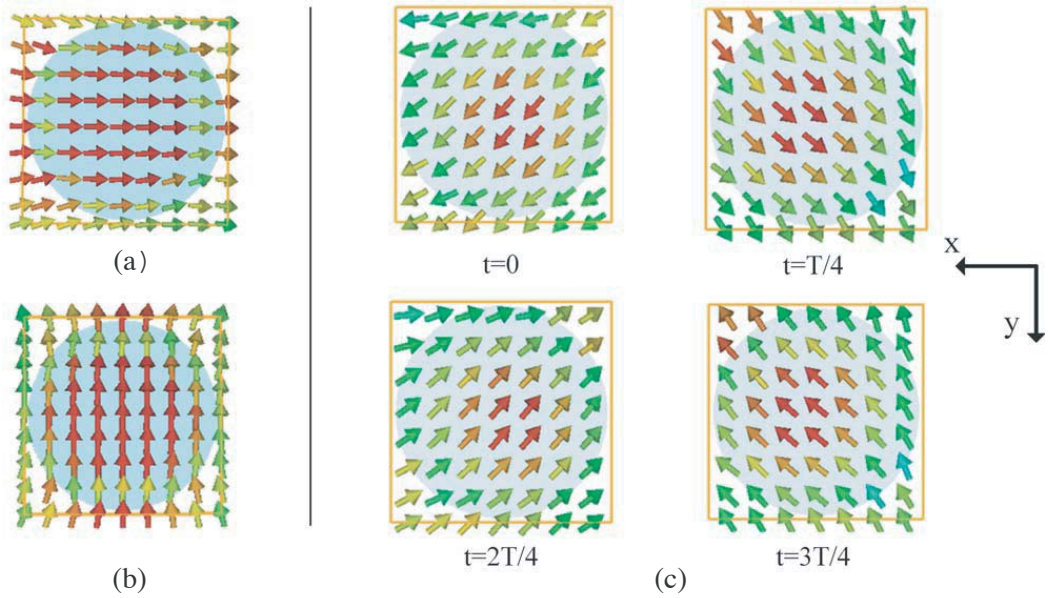

Figure 9. Electric field distributions in the designed antenna: (a) linear horizontal polarization; (b) linear vertical polarization; (c) circular polarization at different time steps.

coupling slots have different lengths, in order to ensure the 90° electrical phase difference at 3.25 GHz necessary for CP operation. The size of the ground plane is 14 cm × 22 cm. The field distributions for LVP, LHP and CP generated by the final designed circuit are presented in Fig. 9. The rotation of electric fields for the circular polarization in one cycle (T) indicates a right hand circular polarization (RHCP), Fig. 9(c). The reflection coefficients for LVP, LHP and CP of the final prototype are shown in Fig. 10. The common bandwidth where the antenna has a measured return loss greater than 10 dB for the three polarization states is measured from 3.05 GHz to 3.6 GHz which is 17%. Fig. 11 shows the 3-dB axial ratio bandwidth of the circular polarization expanding from 3.08 GHz to 3.48 GHz which is

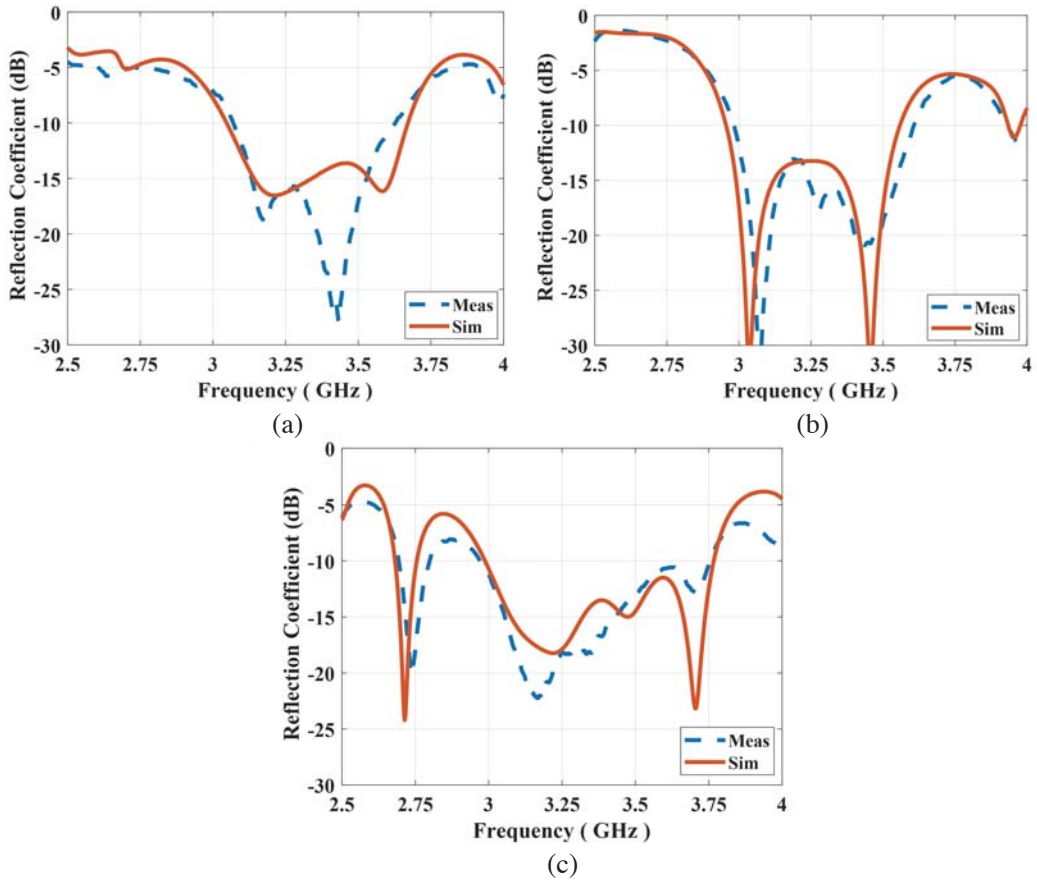

Figure 10. Comparison between measured and simulated reflection coefficients: (a) horizontal linear polarization; (b) vertical linear polarization; (c) circular polarization.

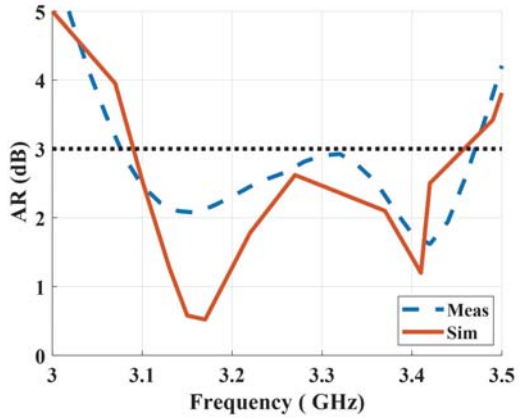

Figure 11. Axial ratio of the circular polarized DRA.

about 12%. Table 2 compares the designed antenna specifications with several reported reconfigurable polarization DRAs.

The designed antenna radiates in broadside direction over its frequency band. The normalized measured patterns of the antenna for different polarizations at the frequency of 3.25 GHz are shown in Fig. 12, showing good agreement with simulated results. The simulated and measured realized gains for the CP, LHP, and LVP polarizations are presented in Fig. 13. If we add the diode losses obtained

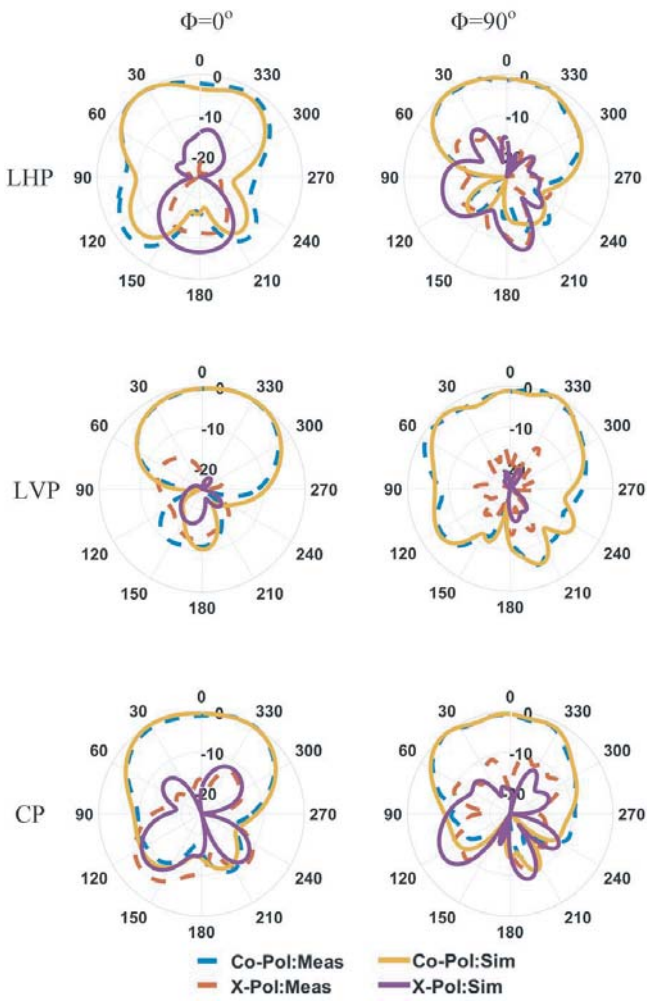

Figure 12. Measured and simulated normalized Co-pols and X-pols for LHP, LVP, and RHCP at 3.25 GHz.

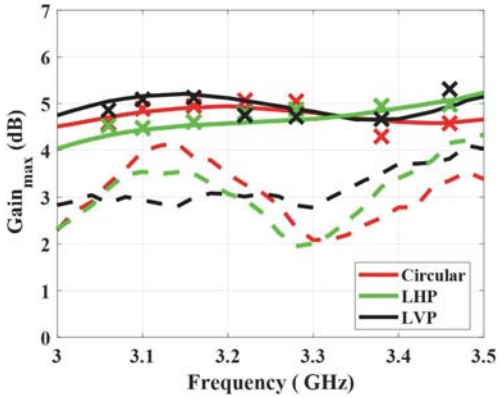

Figure 13. The gain of the reconfigurable DRA for different polarizations; (−) simulations, (- -) measurements, (+) measurements, (×) diode losses.

from Figs. 7(a) and 7(b) to the measured results, we will have a good match between simulated and measured results, as shown in Fig. 13. A better diode and a better diode model is needed to improve the design.

Table 2. State-of-the-art reconfigurable polarization dielectric resonator antennas.

	Reconfigurablity Mechanism	Speed	Polarization States	Number of Diodes	AR Bandwidth	Overlapped Bandwidth
Ref. [11]	Electronically	fast	Two LPs Two CPs	8	6.3%	6.3%
Ref. [12]	Mechanically	slow	Three LPs No CPs	-	-	18%
Ref. [13]	Electronically	fast	Three LPs No CPs	4	-	15%
Ref. [14]	Electronically	fast	Two LPs Two CPs	8	14%	5%
Ref. [10]	Electronically	fast	Two LPs One CPs	2	4%	3%
This Work	Electronically	fast	Two LPs One CPs	2	12%	12%

5. CONCLUSION

In this paper, a new method is introduced to design a reconfigurable polarization cylindrical dielectric resonator antenna. The special way of including the PIN diodes as switching elements in the feeding circuit eliminates the effect of parasitic elements of the diodes on the matching and axial ratio bandwidth of the antenna. Diode losses were found to be the dominant source of discrepancies between measured and simulated gains. Compared to previous electronically controlled concepts allowing at least three polarization states, the proposed design offers improved overlapped return loss and axial ratio bandwidths, a simpler topology, and the smallest number of diodes.

REFERENCES

1. Sharma, Y., D. Sarkar, K. Saurav, and K. V. Srivastava, "Three-element MIMO antenna system with pattern and polarization diversity for WLAN applications," *IEEE Antennas Wireless Propag. Lett.*, Vol. 16, 1163–1166, 2017.
2. Mak, K. M., H. W. Lai, K. M. Luk, and K. L. Ho, "Polarization reconfigurable circular patch antenna with a C-shaped," *IEEE Trans. Antennas Propag.*, Vol. 65, No. 3, 1388–1392, 2017.
3. Zhang, L., S. Gao, Q. Luo, P. R. Young, and Q. Li, "Wideband loop antenna with electronically switchable circular polarization," *IEEE Antennas Wireless Propag. Lett.*, Vol. 16, 242–245, 2017.
4. Bhattacharjee, A., S. Dwari, and M. K. Mandal, "Polarization-reconfigurable compact monopole antenna with wide effective bandwidth," *IEEE Antennas Wireless Propag. Lett.*, Vol. 18, No. 5, 1041–1045, 2019.
5. Shi, Y., Y. Cai, X. Zhang, and K. Kang, "A simple tri-polarization reconfigurable magneto-electric dipole antenna," *IEEE Antennas Wireless Propag. Lett.*, Vol. 17, No. 2, 291–294, 2018.
6. Lee, S. W. and Y. J. Sung, "Simple polarization-reconfigurable antenna with T-shaped feed," *IEEE Antennas Wireless Propag. Lett.*, Vol. 15, 114–117, 2016.
7. Row, J. and Y. Wei, "Wideband reconfigurable crossed-dipole antenna with quad-polarization diversity," *IEEE Trans. Antennas Propag.*, Vol. 66, No. 4, 2090–2094, 2018.
8. Seo, D., J. Kim, M. M. Tentzeris, and W. Lee, "A quadruple-polarization reconfigurable feeding network for UAV RF sensing antenna," *IEEE Microw. Wireless Compon. Lett.*, Vol. 29, No. 3, 183–185, 2019.
9. Lin, W. and H. Wong, "Wideband circular-polarization reconfigurable antenna with L-shaped feeding probes," *IEEE Antennas Wireless Propag. Lett.*, Vol. 16, 2114–2117, 2017.

10. Drossos, G., Z. Wu, and L. E. Davis, "Switchable cylindrical dielectric resonator antenna," *Electron. Lett.*, Vol. 32, No. 10, 862–864, 1996.
11. Liu, B., J. Qiu, C. Wang, W. Li, and G. Li, "Polarization-reconfigurable cylindrical dielectric resonator antenna excited by dual probe with tunable feed network," *IEEE Access*, Vol. 7, 60111–60119, 2019.
12. Chen, Z., H. Wong, and J. Kelly, "A polarization-reconfigurable glass dielectric resonator antenna using liquid metal," *IEEE Trans. Antennas Propag.*, Vol. 67, No. 5, 3427–3432, 2019.
13. Chen, Z., H. Wong, and Y. Liu, "A polarizer integrated dielectric resonator antenna for polarization reconfigurability," *IEEE Trans. Antennas Propag.*, Vol. 67, No. 4, 2723–2728, 2019.
14. Liu, B., J. Qiu, C. Wang, N. Wang, and G. Li, "Rectangular dielectric resonator antenna with polarization reconfigurable characteristic," *Microwave Opt. Technol. Lett.*, Vol. 61, 766–771, 2018.
15. Blais-Morin, L. A. and J. J. Laurin, "Low insertion loss hybrid pin diode switches in Ku and Ka bands," *Microwave Opt. Technol. Lett.*, Vol. 28, No. 1, 28–32, 2001.
16. Fang, X. S. and K. W. Leung, "Linear-/circular-polarization designs of dual-/wide-band cylindrical dielectric resonator antennas," *IEEE Trans. Antennas Propag.*, Vol. 60, No. 6, 2662–2671, 2012.
17. Zhang, L., S. Gao, Q. Luo, P. R. Young, and Q. Li, "Wideband loop antenna with electronically switchable circular polarization," *IEEE Antennas Wireless Propag. Lett.*, Vol. 16, 242–245, 2017.